Article

Unilateral Cleavage Furrows in Multinucleate Cells

Julia Bindl [1], Eszter Sarolta Molnar [1], Mary Ecke [1], Jana Prassler [1], Anette Müller-Taubenberger [2] and Günther Gerisch [1,*]

[1] Max Planck Institute of Biochemistry, Am Klopferspitz 18, D-82152 Martinsried, Germany; J.bindl@campus.lmu.de; eszter.molnar@campus.lmu.de; ecke@biochem.mpg.de; prassler@biochem.mpg.de; gerisch@biochem.mpg.de

[2] LMU Munich, Department of Cell Biology (Anatomy III), Biomedical Center, D-82152 Planegg-Martinsried, Germany; amueller@bmc.med.lmu.de

* Correspondence: gerisch@biochem.mpg.de; Tel.: +49 89 8578-2326

Abstract: Multinucleate cells can be produced in *Dictyostelium* by electric-pulse induced fusion. In these cells unilateral cleavage furrows are formed at spaces between areas that are controlled by aster microtubules. A peculiarity of unilateral cleavage furrows is their propensity to join laterally with other furrows into rings to form constrictions. This means, cytokinesis is biphasic in multinucleate cells, the final abscission of daughter cells being independent of the initial direction of furrow progression. Myosin-II and the actin-filament cross-linking protein cortexillin accumulate in the unilateral furrows, as they do in the normal cleavage furrows of mononucleate cells. Myosin-II is not essential for cytokinesis, but stabilizes and confines the position of the cleavage furrows.

Keywords: cell fusion; cortexillin; cytokinesis; *Dictyostelium*; myosin

1. Introduction

Mitotic cell division is typically mediated by a contractile ring that after segregation of the chromosomes separates two halves of the cell by a cleavage furrow. Constriction of the ring is based on the interaction of anti-parallel myosin-II filaments with actin filaments that are linked to the membrane [1]. Cells of the eukaryotic microorganism *Dictyostelium discoideum* are no exceptions in the sense that myosin-II is accumulating in the furrow region [2], and that cytokinesis is impaired in myosin-II-null mutants [3-5]. However, cytokinesis is strongly inhibited only when cells are cultivated in suspension. When attached to an adhesive substrate surface, the mutant cells are capable of forming a cleavage furrow, albeit less efficiently than wild-type cells [6].

A protein required for cytokinesis in *D.discoideum* is cortexillin that causes anti-parallel bundling of actin filaments [7]. Three isoforms, cortexillin I to III, form preferentially heterodimers [8, 9]. Cortexillin accumulates in the cleavage furrow, independently of myosin-II [9-11]. Cells lacking both cortexillins I and II are severely impaired in cytokinesis [7].

Subject of the present report is the formation of unilateral cleavage furrows in multinucleate cells. In myosin-II-null mutants, multinucleate cells have been produced by growth in suspension. Under these conditions, nuclei divide synchronously but cytokinesis is impaired. To study cytokinesis, the large cells are transferred to an adhesive substrate surface, where they form multiple cleavage furrows ingressing from their border [6]. The sites of these unilateral furrows are negatively controlled by positioning of the microtubule asters that emanate from the centrosomes during mitosis. The aster microtubules induce the cell cortex to ruffle, thus preventing the formation of a furrow. The cells are cleaved at spaces between asters, even if the flanking asters are not connected by a spindle [12].

Here we compare cytokinesis in multinucleate wild-type cells of *D. discoideum*, produced by electric-pulse induced fusion [13], with cytokinesis in myosin-II-null cells. In the wild-type cells, the accumulation of GFP-tagged myosin-II is visualized in unilateral furrows, in myosin-II-null cells the accumulation of GFP-cortexillin.

 doi:10.20944/preprints202002.0322.v1

2. Materials and Methods

2.1. Cell strains and culture conditions

Fluorescent proteins were expressed in the AX2-214 strain of *D. discoideum* or in the HS2205 strain derived from it. In HS2205, myosin-II heavy chains have been deleted [5]. In the AX2-214 strain, either GFP-myosin-II [14] together with mRFPM-α-tubulin [15], GFP-α-tubulin [12] together with mRFP1-histone 2B, or mRFPM-LimEΔ [15] together with GFP-α-tubulin were expressed. In the HS2205 strain, GFP-cortexillin I [16] was expressed together with mRFPM-histone 2B.

2.2. Design of mRFP-histone 2B vectors

For the expression of histone 2B C-terminally of mRFP, two vectors were constructed, one conferring resistance to blasticidin, the other to hygromycin. For blasticidin, the coding sequence of the *D. discoideum* histone variant H2Bv3 (DDB0231622|DDB_G0286509) was cloned into the *Eco*RI-site 3′ of mRFP1 [17] and expressed under control of an actin-15 promoter, using a pDEX-based vector conferring resistance to blasticidin [18].

To construct an expression vector with a hygromycin selection marker [19], the cassette A15P-mRFPmars-A8T consisting of actin-15 promoter, mRFPmars coding region [15], and actin-8 terminator was cloned between the *Sma*I and *Sph*I sites of the multiple cloning site of the pGEM7-based plasmid pHygTm(plus)/pG7 (a kind gift of Jeff Williams and Masashi Fukuzawa, University of Dundee). Subsequently, the coding sequence of histone H2Bv3 was inserted into the *Eco*RI site 3′ of mRFPmars.

2.3. Culture conditions and sample preparation for confocal microscopy

Cells were cultivated in Petri dishes containing nutrient medium [20] supplemented with 10 µg / ml of Blasticidin S (Gibco, Life Technologies Corporation, Grand Island, NY, USA), 10 µg / ml of Geneticin (Sigma-Aldrich, St. Louis, MO, USA) or of 33 µg / ml Hygromycin B (EMD Millipore Corp., Billerica, MA, USA) at 21±2°C.

For imaging, cells rinsed off the Petri dish were transferred to an HCl-cleaned cover-glass bottom dish (FluoroDish, WPI INC., Sarasota, FL, USA) and kept for 1 to 2 hours in LoFlo medium (ForMedium Ltd., Norfolk, UK). The rate of mitosis could be increased by incubating the cells for about 20 hours at 4°C in Petri dishes with nutrient medium and subsequently bringing them to room temperature before transfer to LoFlo medium.

Large cells with wild-type AX2-214 background were produced by electric-pulse induced fusion as described by [13]. Myosin-II-null cells were cultivated in shaken suspension in nutrient medium for about 36 hours to get large multinucleate cells [6]. Multinucleate cells were transferred onto HCl-cleaned cover-glass bottom dishes and incubated in LoFlo medium for about 1 hour before imaging was started. For imaging the microtubule arrays, cells were overlaid with a thin agarose sheet [21, 22] as indicated in the figure legends.

2.4. Confocal image acquisition and data processing

For confocal images a Zeiss LSM 780 microscope equipped with a Plan-Apo 63x/NA 1.46 oil immersion objective was used (Zeiss AG, Oberkochen, Germany). Images were processed using the image-processing package Fiji (http://Fiji.sc/Fiji) developed by [23] on the basis of ImageJ (http://imagej.nih.gov/ij). For bleach correction of the red channel the total mean grey level for each image of a series was measured to calculate the percentage of bleaching and accordingly the brightness of the red channel was linearly enhanced.

For 3D rendering and animation the images were first deconvolved with the software of Huygens Essential, version 18.04 (Scientific Volume Imaging b.v., Hilversum, The Netherlands) and then animated and displayed in UCSF Chimera, version 1.14 (https://www.cgl.ucsf.edu/chimera) [24].

 doi:10.20944/preprints202002.0322.v1

3. Results

3.1. Mitotic cell division in mononucleate cells

As a reference for the mitotic division of multinucleate cells, we first show spindle dynamics, chromosome segregation, and cleavage furrow formation in cells containing a single dividing nucleus. The cell in Figure 1A and Video 1 expressed GFP-α-tubulin (green) as a constituent of the mitotic apparatus together with mRFP-histone 2B as a label of the chromosomes (red). During metaphase (0-s frame), the two centrosomes stay at a distance of only 2 µm from each other. Accordingly short is the connecting spindle, which subsequently elongates within 3 minutes to a length of up to 13 µm, before it disrupts in the middle. At anaphase, the two sets of daughter chromosomes immediately follow the separating centrosomes, which means that the centromere-associated microtubules remain short. During the entire process, aster microtubules connect the centrosomes with the polar regions of the cell cortex. Not seen in Figure 1 is the nuclear membrane, which separates in the semi-closed mitosis of Dictyostelium the centrosomes from the intranuclear spindle [25, 26].

Upon disruption of the spindle, the cleavage furrow ingresses, separating the daughter cells except for a thin tubular bridge that finally is scissioned by a dynamin A dependent mechanism [27]. Filamentous actin is most prominently accumulated in rounded protrusions at the polar regions of the dividing cell, and only faintly in the cleavage furrow (Fig. 1B, Videos 1 and 2).

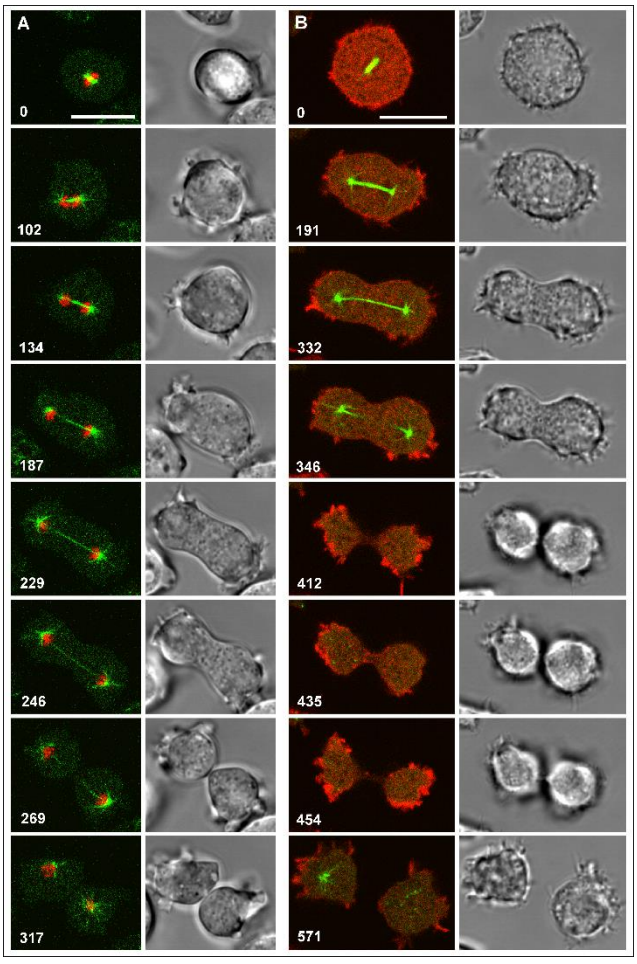

Figure 1. Mitosis and cytokinesis in wild-type cells of Dictyostelium discoideum. Left panels in the time series of (A) and (B) show confocal dual-color fluorescence images, right panels DIC bright-field images. Time after the first frame of each series is indicated in seconds. Scale bar, 10 µm. (**A**) A cell expressing GFP-α-tubulin

 doi:10.20944/preprints202002.0322.v1

as a label for the mitotic apparatus (green) and mRFP-histone 2B to visualize the chromosomes (red). The elongated spindle is disrupted between the 246-s and 269-s frames. The 317-s frame shows in the right cell radial microtubules connecting the centrosome with the cell cortex. (**B**) A cell expressing GFP-α-tubulin (green) and mRFP-LimEΔ as a label for filamentous actin (red). Fluorescence images are primarily focused on the spindle or on polar protrusions; for the 435-s frame the focus has been changed to the cleavage furrow, where little actin is accumulated. The cell has been flattened by agarose overlay. The same sequence is shown in supplemental Video 1. For a 3D display showing polar protrusions attached to the substrate surface, see supplemental Video 2.

3.2. Unilateral cleavage furrows in multinucleate wild-type cells

In all kinds of multinucleate cells tested, this means in fused wild-type cells, myosin-II-null cells pre-grown in suspension, and in cortexillin I- and II-null cells, the nuclei divide synchronously. We have studied two proteins that are involved in cleavage furrow formation accompanying mitosis in multinucleate cells, the two-headed motor protein myosin-II [14] and cortexillin, which is an anti-parallel bundler of actin filaments [7].

The division of large wild-type cells produced by electric-pulse induced fusion is exemplified in Figure 2 and Video 3 showing a cell that expressed mRFP-α-tubulin to label the mitotic apparatus, together with

GFP-myosin-II heavy-chains to visualize accumulation of the myosin in unilateral furrows. The mitotic apparatus shows the docking of aster microtubules to the cell cortex as previously observed in myosin-II-null cells [6]. The docking results in bending of the spindle (15-s frame) and in the induction of protrusions where furrow formation is inhibited. Again in accord with previous findings on myosin-II-null cells [12], furrows ingress at spaces not occupied by microtubule asters, independent of whether or not these spaces are bridged by a spindle.

Preprints (www.preprints.org) | NOT PEER-REVIEWED | Posted: 23 February 2020 doi:10.20944/preprints202002.0322.v1

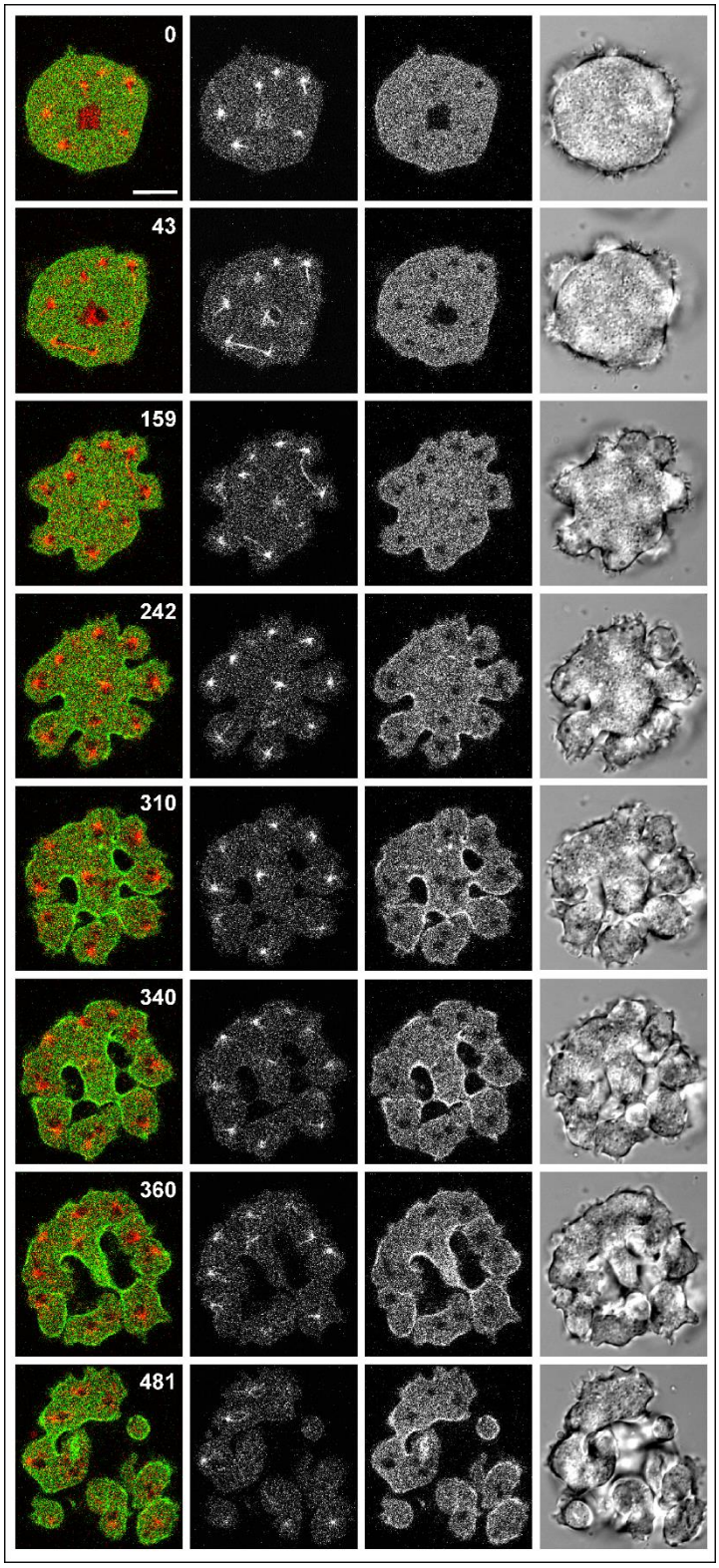

Figure 2. Multinucleate wild-type cell produced by electric-pulse induced fusion. The cells fused expressed mRFP-α-tubulin (red) and GFP-myosin-II heavy chains (green in the merged panels). Confocal fluorescence images show the labels merged but also separate. In the α-tubulin panels, a straight spindle before furrow ingression, and a spindle bent after the onset of furrowing are indicated by arrowheads. Time is indicated in seconds after the first frame. Scale bar, 10 μm. The entire time series from which the images of Figure 2 are taken, is covered in Video 3.

Preprints (www.preprints.org) | NOT PEER-REVIEWED | Posted: 23 February 2020 doi:10.20944/preprints202002.0322.v1

The unilateral furrows in wild-type cells widen during ingression (Fig. 3A) and tend to cooperate with neighboring furrows to form constricting rings that separate mono- or oligo-nucleate portions from the multinucleate cell mass (Fig. 3B). These cases are of interest because here the final constriction is not a continuation of the initial furrow ingression but proceeds laterally between two furrows.

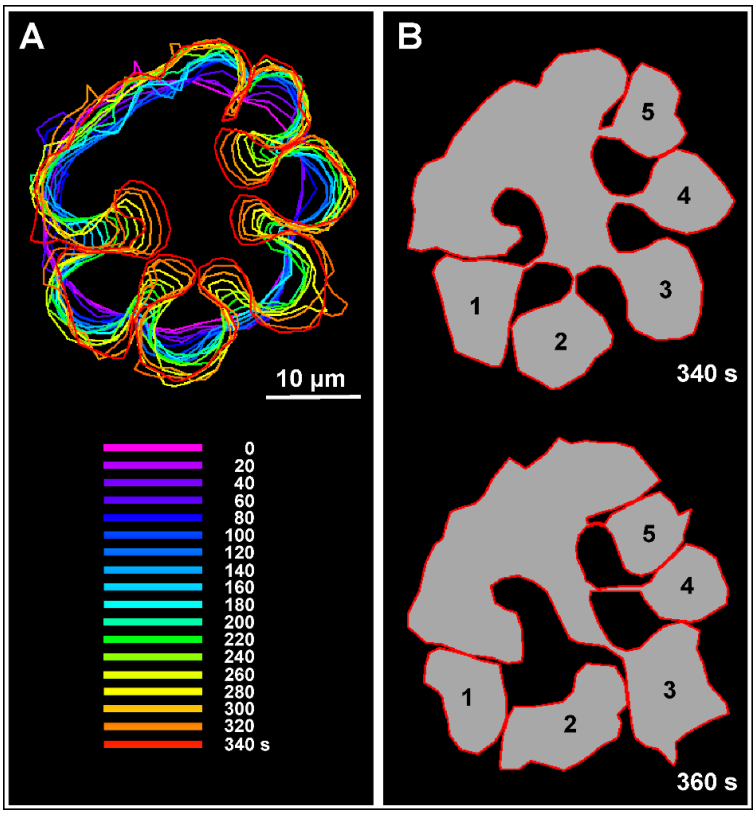

Figure 3. Progression of cleavage furrows in the multinucleate cell of Figure 2. (**A**) Color-coded cell boundaries within the 0 to 360-s time span derived from the confocal fluorescence images of myosin-II. (**B**) Comparison of cell boundaries at the 340-s and 360-s time points. These drawings show cell shapes in the confocal plane, with additional information on connectivity gathered from the bright-field images. Within the time span of 20 s the daughter cells 1 and 2 became disconnected while abscission of the incipient daughter cells 3 to 5 proceeded. In all these cases abscission occurred obliquely to the initial furrowing.

3.3 Division of mononucleate and multinucleate myosin-II-null cells

The inability of myosin-II-null cells to perform cytokinesis in suspension and the support of their mitotic division by an adhesive substrate made it easy to compare mononucleate and multinucleate cells in the absence of myosin-II. The majority of mononucleate myosin-II-null cells attached to a substrate surface complete cytokinesis, accumulating cortexillin in the cleavage furrow (Fig. 4A and Video 4). Instability of positioning the furrow is indicated by those cells in which the furrow, initiated as usual in the middle of the cell, slips to one side such that it would separate a binucleate portion from an anucleate one (Fig. 4B and Video 4). In that way the furrow becomes located on top of aster microtubules, which do not support further ingression. The anucleate portion is rather retracted, resulting in failure of cytokinesis.

Preprints (www.preprints.org) | NOT PEER-REVIEWED | Posted: 23 February 2020 doi:10.20944/preprints202002.0322.v1

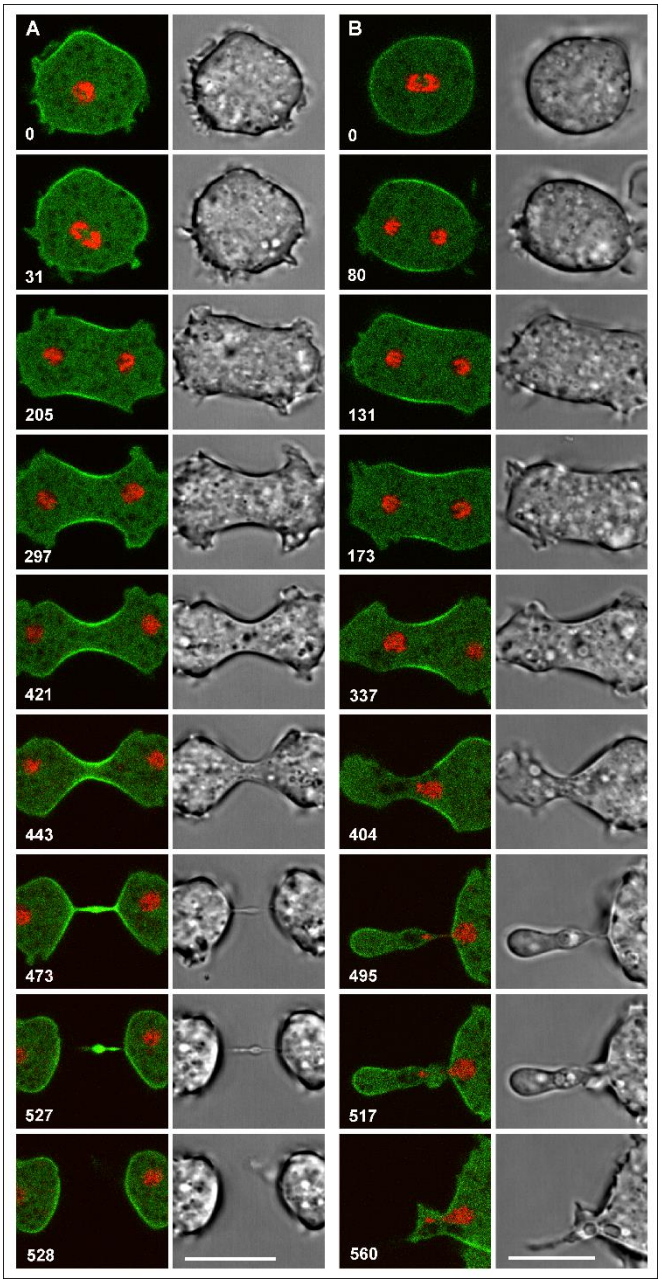

Figure 4. Successful and failing cytokinesis in myosin-II-null cells. Mitoses of mononucleate cells on a glass surface are shown in confocal fluorescence (left panels) and bright field images (right panels). The cells expressed GFP-cortexillin I (green), together with mRFP-histone 2B as a label of the chromosomes. Time is indicated in seconds after the first frame. Scale bar, 10 μm. The entire sequences of (A) and (B) are shown in supplemental Video 4. (**A**) Successful cell division showing cortexillin accumulating in the cleavage furrow that divides the cell between the two daughter nuclei.(**B**) Unsuccessful cytokinesis, which begins like the successful one with the accumulation of cortexillin in the midzone. However, subsequently the furrow becomes asymmetric and the left nucleus slips toward the right, the now anucleate part of the cell becoming integrated into the binucleate one. The cell has been flattened by agarose overlay.

 doi:10.20944/preprints202002.0322.v1

Multinucleate myosin-II-null cells can divide by unilateral furrows to which cortexillin is localized. However, these mutant cells appear to inefficiently restrict expansion of these furrows. An extreme example is shown in Figure 5 and Video 5, where furrows strongly expand before daughter cells are separated. The multinucleate cell shown in Figure 6 and Video 6 also forms a long furrow (by arrowhead indicated as furrow 1), which in cooperation with furrow 2 gives rise to a daughter cell, while interaction with furrow 3 fails: all three nuclei in the incipient daughter cell slip through the furrow into the major part of the cell (774-s and 936-s frames). The anucleate remnant directs protrusions toward the major part (996-s frame) and reintegrates, similar to the anucleate portion of the mitotic cell in Figure 4B.

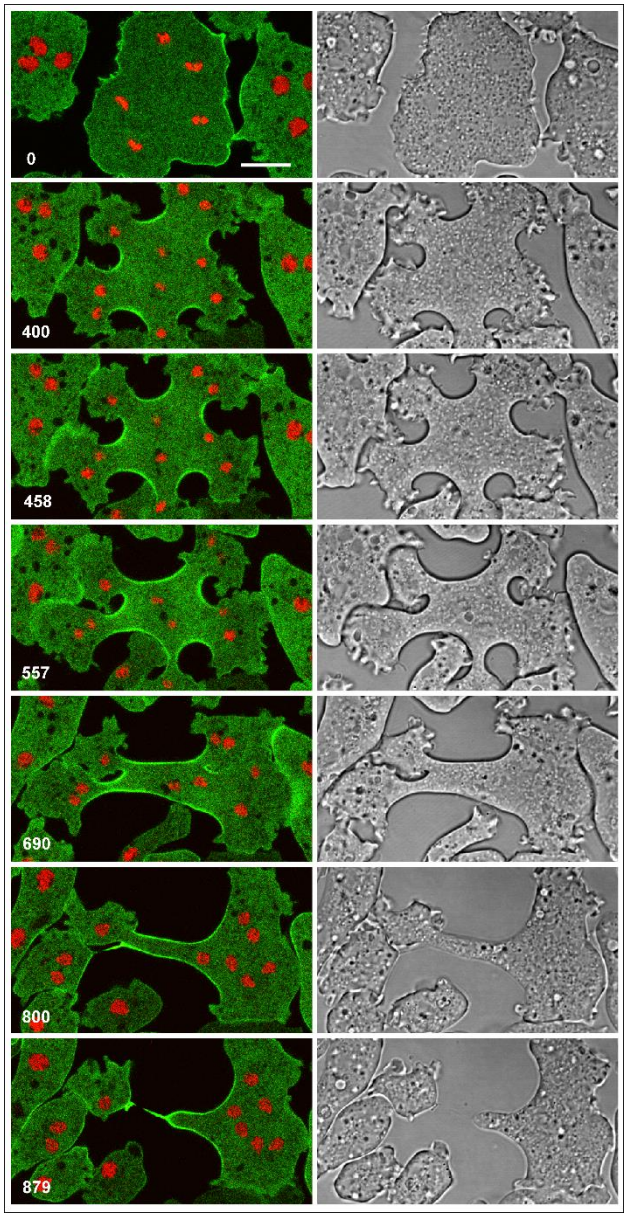

Figure 5. Synchronous mitosis and division of a multinucleate myosin-II-null cell. As the cells in Figure 4, this cell expressed GFP-cortexillin I (green) and mRFP-histone 2B (red). Initially five unilateral furrows formed that were enriched in cortexillin (400-s to 557-s frames). Later on, two long furrows prevailed (690-s and 800-s frames), and a final abscission occurred between them (879-s frame). The cell has been flattened by agarose overlay. Time is indicated in seconds after the first frame. Scale bar, 10 μm. The entire sequence is shown in supplemental Video 5.

Preprints (www.preprints.org) | NOT PEER-REVIEWED | Posted: 23 February 2020 doi:10.20944/preprints202002.0322.v1

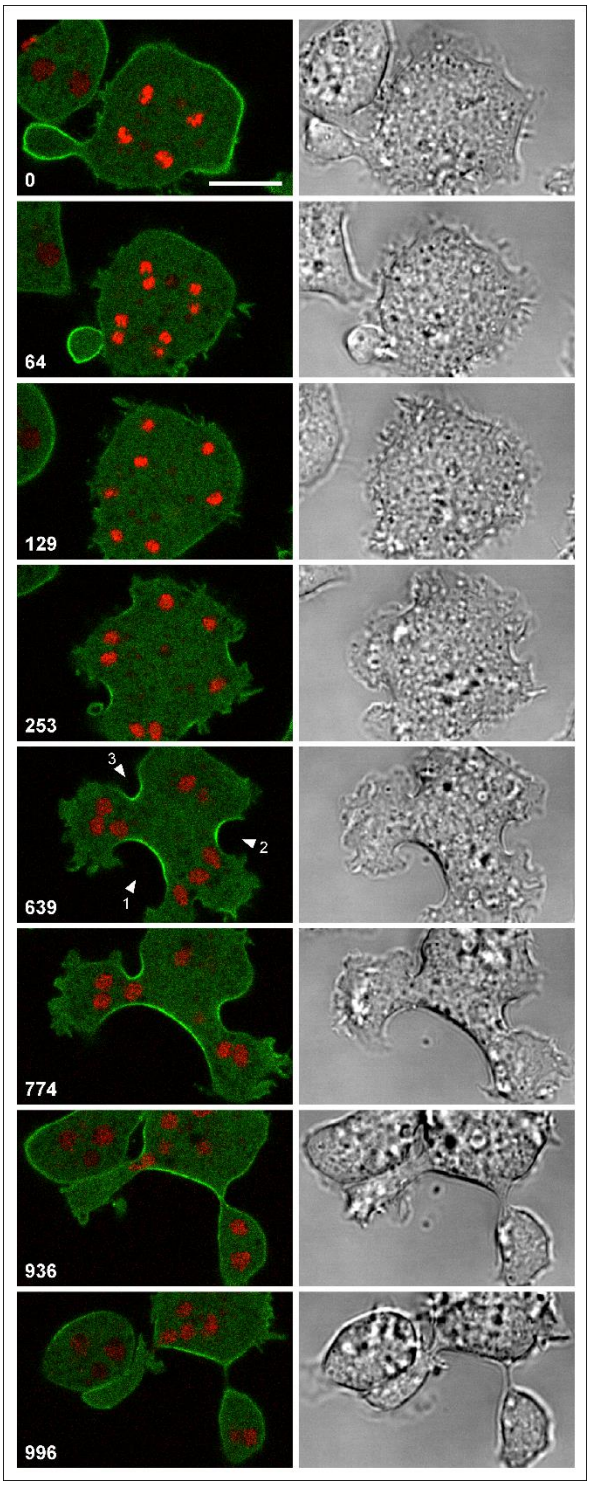

Figure 6. A multinucleate myosin-II-null cell labeled, as the cell in Figure 5, for cortexillin I (green) and for the chromosomes (red). Three unilateral furrows are indicated by arrowheads in the 639-s frame. Between furrow 1 and 2 abscission of a daughter cell proceeds, whereas between furrows 1 and 3 three nuclei slip from the left portion into the major cell body (774-s and 936-s frames). Consequently, the anucleate part is united with the major cell body, forming protrusions toward the latter (open arrowhead in the 996-s frame). Time is indicated in seconds after the first frame. Scale bar, 10 μm. The same sequence is shown in supplemental Video 6.

 doi:10.20944/preprints202002.0322.v1

4. Discussion

There are examples of unilateral cleavage furrows in cells other than the multinucleate *Dictyostelium* cells. Such furrows have been observed in somatic mammalian cells (electro-fused PtK1 cells) [28]. During meiosis II in mouse oocytes, a unilateral furrow initiates polar body formation [29]. After turning of the spindle, this furrow is converted into a bilateral one or a contractile ring (reviewed by [30]). Related to unilateral furrowing is the ingression of furrows between the nuclei during blastoderm formation in early insect embryogenesis [31]. The subsequent constriction of a ring on the blastoderm-yolk interface occurs in two steps: a slow first phase is myosin-II dependent, not however a second faster phase [32].

In *D.discoideum*, myosin-II-null as well as wild-type cells provide the possibility of studying the division of mononucleate and multinucleate cells, and thus of normal and unilateral cleavage furrow formation, in an identical genetic background. In the myosin-II-null background, cells grown in suspension or on an adhesive substrate are compared; whereas in the wild-type background, multinucleate cells are produced by electric-pulse induced fusion.

Both wild-type and myosin-II-null cells show how two unilateral furrows join to form a ring that separates a daughter cell from the multinucleate cell body (Figs. 2 and 3). In myosin-II-null cells, this ring is constricting by a myosin-II independent mechanism. The data obtained in mononucleate and multinucleate myosin-II-null cells are in accord with previous findings indicating that myosin-II stabilizes the position of the cleavage furrow [11, 33], preventing its lateral sliding (Fig. 4B) or expansion (Figs. 5 and 6).

The ingression of cleavage furrows between centrosomes that are not connected by a spindle relates the cytokinesis in multinucleate *Dictyostelium* cells to furrows in sand dollar eggs [34]. However, Rappaport [35] argued that these furrows are induced by aster microtubules, whereas in *Dictyostelium* the membrane areas associated with asters form actin-rich protrusions rather than ingressing furrows ([6, 12] and Figure 2 of the present paper). There is in the multinucleate cells no recognizable microtubule structure in spindle-free inter-centrosomal spaces that may act as a source of signals for furrow ingression.

A protein important for the formation of cleavage furrows in *Dictyostelium* is cortexillin, which bundles actin-filaments [7]. Cortexillin may serve a function similar to anillin, another actin-bundling protein [36, 37], which is missing in *Dictyostelium*. In various other cells, the anillin is recruited to the furrow region to fulfill multiple functions in cytokinesis [38]. In vitro, anillin can be shown to act independently of myosin in the constriction of an actin ring [39].

The unilateral furrows studied here indicate that for initiation of a cleavage furrow no contractile ring is required. The accumulation of myosin-II and cortexillin in the unilateral furrows formed in multinucleate wild-type cells indicates that these furrows are produced by the same molecular machinery as ring-shaped furrows in mononucleate cells.

5. Conclusions

Peculiar to cytokinesis in the multinucleate cells of *Dictyostelium* is the variable geometric relationship between furrow ingression and the subsequent ring contraction that finally results in abscission of daughter cells (Fig. 3). Ring formation may just be a continuation of initial ingression. This is the case when two furrows meet each other from opposite sides (Fig. 7A). However, different from cytokinesis in mononucleate cells, the rings may also be formed laterally of the initial ingression (Fig. 7B), thus separating the entire process of cleavage into two distinct phases.

Preprints (www.preprints.org) | NOT PEER-REVIEWED | Posted: 23 February 2020 doi:10.20944/preprints202002.0322.v1

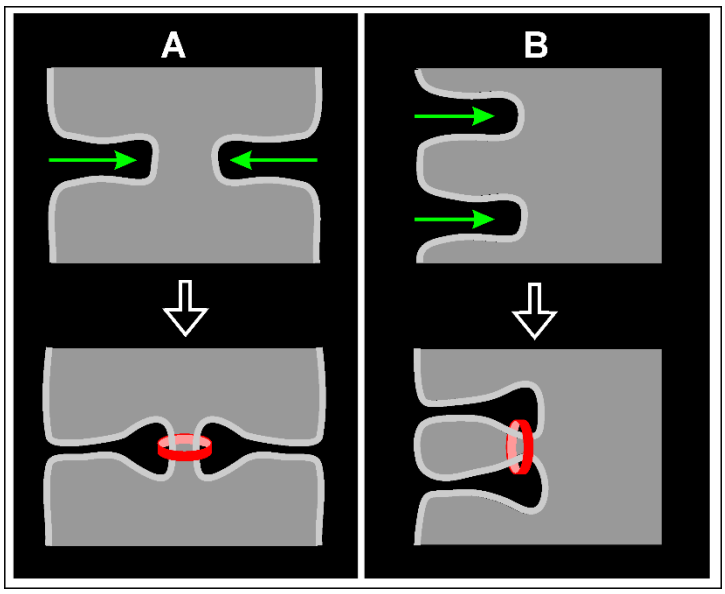

Figure 7. Diagram of cytokinesis in multinucleate cells, illustrating the variable spatial relationship of initial furrow ingression (green arrows) and final abscission (red ring). **(A**) Two furrows ingressing from opposite sides and abscission proceeding in continuation of the furrow directions. (**B**) Two furrows ingressing in parallel directions and abscission occurring obliquely to these directions.

Supplementary Materials: The following are available online, Video 1: Mitosis and cytokinesis in a wild-type cell of *Dictyostelium discoideum*, Video 2: Animation of three stages of cell division of a 3D rendered wild-type cell of *D. discoideum*, Video 3: A multinucleate wild-type cell produced by electric-pulse induced fusion, Video 4: Successful (top) and failing (bottom) cytokinesis in myosin-II-null cells, Video 5: Synchronous mitosis and division of a multinucleate myosin-II-null cell, Video 6: A multinucleate myosin-II-null cell.

Author Contributions: Conceptualization, Günther Gerisch; Data curation, Julia Bindl, Eszter Sarolta Molnar, Mary Ecke, Jana Prassler and Günther Gerisch; Formal analysis, Julia Bindl, Eszter Sarolta Molnar, Mary Ecke and Jana Prassler; Investigation, Julia Bindl, Eszter Sarolta Molnar, Mary Ecke, Jana Prassler and Annette Müller-Taubenberger; Project administration, Günther Gerisch; Supervision, Günther Gerisch; Visualization, Eszter Sarolta Molnar, Mary Ecke and Jana Prassler; Writing – original draft, Günther Gerisch.

Funding: This work was funded by the Max Planck Society to G. G.

Acknowledgments: We thank Martin Spitaler and his team at the Imaging Facility of the Max Planck Institute of Biochemistry for cooperation and providing the software Huygens Essential, Petra Fey and dictyBase for providing information [40].

Conflicts of Interest: The authors declare no competing or financial interests.

References

1. Pollard, T. D.; O'Shaughnessy, B., Molecular mechanism of cytokinesis. *Annu. Rev. Biochem.* **2019,** *88* (1), 661-689.
2. Fukui, Y.; Inoue, S., Cell division in Dictyostelium with special emphasis on actomyosin organization in cytokinesis. *Cell Motil Cytoskel* **1991,** *18*, 41-54.
3. De Lozanne, A.; Spudich, J. A., Disruption of the Dictyostelium myosin heavy chain gene by homologous recombination. *Science* **1987,** *236* (4805), 1086-1091.
4. Knecht, D. A.; Loomis, W. F., Antisense RNA inactivation of myosin heavy chain gene expression in Dictyostelium discoideum. *Science* **1987,** *236*, 1081-1085.
5. Manstein, D. J.; Titus, M. A.; De Lozanne, A.; Spudich, J. A., Gene replacement in Dictyostelium: generation of myosin null mutants. *EMBO J.* **1989,** *8* (3), 923-932.

6. Neujahr, R.; Heizer, C.; Gerisch, G., Myosin II-independent processes in mitotic cells of Dictyostelium discoideum: redistribution of the nuclei, re-arrangement of the actin system and formation of the cleavage furrow. *J. Cell Sci.* **1997,** *110* (2), 123.
7. Faix, J.; Steinmetz, M.; Boves, H.; Kammerer, R. A.; Lottspeich, F.; Mintert, U.; Murphy, J.; Stock, A.; Aebi, U.; Gerisch, G., Cortexillins, major determinants of cell shape and size, are actin-bundling proteins with a parallel coiled-coil tail. *Cell* **1996,** *86*, 631-642.
8. Faix, J.; Weber, I.; Mintert, U.; Köhler, J.; Lottspeich, F.; Marriott, G., Recruitment of cortexillin into the cleavage furrow is controlled by Rac1 and IQGAP-related proteins. *EMBO J.* **2001,** *20* (14), 3705-3715.
9. Liu, X.; Shu, S.; Yu, S.; Lee, D.-Y.; Piszczek, G.; Gucek, M.; Wang, G.; Korn, E. D., Biochemical and biological properties of cortexillin III, a component of Dictyostelium DGAP1–cortexillin complexes. *Mol Biol Cell* **2014,** *25* (13), 2026-2038.
10. Gerisch, G.; Weber, I., Cytokinesis without myosin II. *Curr. Opin. Cell Biol.* **2000,** *12* (1), 126-132.
11. Weber, I.; Neujahr, R.; Du, A.; Köhler, J.; Faix, J.; Gerisch, G., Two-step positioning of a cleavage furrow by cortexillin and myosin II. *Curr. Biol.* **2000,** *10* (9), 501-506.
12. Neujahr, R.; Albrecht, R.; Köhler, J.; Matzner, M.; Schwartz, J. M.; Westphal, M.; Gerisch, G., Microtubule-mediated centrosome motility and the positioning of cleavage furrows in multinucleate myosin II-null cells. *J. Cell Sci.* **1998,** *111* (9), 1227.
13. Gerisch, G.; Ecke, M.; Neujahr, R.; Prassler, J.; Stengl, A.; Hoffmann, M.; Schwarz, U. S.; Neumann, E., Membrane and actin reorganization in electropulse-induced cell fusion. *J. Cell Sci.* **2013,** *126* (Pt 9), 2069-2078.
14. Robinson, D. N.; Cavet, G.; Warrick, H. M.; Spudich, J. A., Quantitation of the distribution and flux of myosin-II during cytokinesis. *BMC Cell Biol.* **2002,** *3* (1), 4.
15. Fischer, M.; Haase, I.; Simmeth, E.; Gerisch, G.; Müller-Taubenberger, A., A brilliant monomeric red fluorescent protein to visualize cytoskeleton dynamics in Dictyostelium. *FEBS Lett.* **2004,** *577* (1-2), 227-232.
16. Weber, I.; Gerisch, G.; Heizer, C.; Murphy, J.; Badelt, K.; Stock, A.; Schwartz, J. M.; Faix, J., Cytokinesis mediated through the recruitment of cortexillins into the cleavage furrow. *EMBO J.* **1999,** *18* (3), 586-594.
17. Campbell, R. E.; Tour, O.; Palmer, A. E.; Steinbach, P. A.; Baird, G. S.; Zacharias, D. A.; Tsien, R. Y., A monomeric red fluorescent protein. *Proc Natl Acad Sci* **2002,** *99* (12), 7877.
18. Müller-Taubenberger, A., Application of fluorescent protein tags as reporters in live-cell imaging studies. In *Dictyostelium discoideum Protocols*, Eichinger, L.; Rivero, F., Eds. Humana Press: Totowa, NJ, 2006; Vol. 346, pp 229-246.
19. Gritz, L.; Davies, J., Plasmid-encoded hygromycin B resistance: the sequence of hygromycin B phosphotransferase gene and its expression in Escherichia coli and Saccharomyces cerevisiae. *Gene* **1983,** *25* (2), 179-188.
20. Malchow, D.; Nägele, B.; Schwarz, H.; Gerisch, G., Membrane-bound cyclic AMP phosphodiesterase in chemotactically responding cells of Dictyostelium discoideum. *Eur. J. Biochem.* **1972,** *28* (1), 136-142.
21. Fukui, Y.; Yumura, S.; Yumura, T. K., Agar-overlay immunofluorescence: high-resolution studies of cytoskeletal components and their changes during chemotaxis. *Methods Cell Biol* **1987,** *28*, 347-356.
22. Samereier, M.; Meyer, I.; Koonce, M. P.; Gräf, R., Live cell-Imaging techniques for analyses of microtubules in Dictyostelium. In *Methods Cell Biol*, Cassimeris, L.; Tran, P., Eds. Academic Press: 2010; Vol. 97, pp 341-357.
23. Schindelin, J.; Arganda-Carreras, I.; Frise, E.; Kaynig, V.; Longair, M.; Pietzsch, T.; Preibisch, S.; Rueden, C.; Saalfeld, S.; Schmid, B., Fiji: an open-source platform for biological-image analysis. *Nat. Methods* **2012,** *9* (7), 676-682.
24. Pettersen, E. F.; Goddard, T. D.; Huang, C. C.; Couch, G. S.; Greenblatt, D. M.; Meng, E. C.; Ferrin, T. E., UCSF Chimera—A visualization system for exploratory research and analysis. *J Comput Chem* **2004,** *25* (13), 1605-1612.
25. Leo, M.; Santino, D.; Tikhonenko, I.; Magidson, V.; Khodjakov, A.; Koonce, M. P., Rules of engagement: centrosome–nuclear connections in a closed mitotic system. *Biol Open* **2012,** *1* (11), 1111.
26. McIntosh, J. R.; Roos, U. P.; Neighbors, B.; McDonald, K. L., Architecture of the microtubule component of mitotic spindles from Dictyostelium discoideum. *J. Cell Sci.* **1985,** *75* (1), 93.

27. Wienke, D. C.; Knetsch, M. L. W.; Neuhaus, E. M.; Reedy, M. C.; Manstein, D. J., Disruption of a dynamin homologue affects endocytosis, organelle morphology, and cytokinesis in Dictyostelium discoideum. *Mol Biol Cell* **1999,** *10* (1), 225-243.
28. Savoian, M. S.; Khodjakov, A.; Rieder, C. L., Unilateral and wandering furrows during mitosis in vertebrates: implications for the mechanism of cytokinesis *Cell Biol. Int.* **1999,** *23* (12), 805-812.
29. Wang, Q.; Racowsky, C.; Deng, M., Mechanism of the chromosome-induced polar body extrusion in mouse eggs. *Cell Div* **2011,** *6* (1), 17.
30. Uraji, J.; Scheffler, K.; Schuh, M., Functions of actin in mouse oocytes at a glance. *J. Cell Sci.* **2018,** *131* (22), jcs218099.
31. Schejter, E. D.; Wieschaus, E., Functional elements of the cytoskeleton in the early Drosophila embryo. *Annu Rev Cell Biol* **1993,** *9* (1), 67-99.
32. Xue, Z.; Sokac, A. M., Back-to-back mechanisms drive actomyosin ring closure during Drosophila embryo cleavage. *J. Cell Biol.* **2016,** *215* (3), 335-344.
33. Neujahr, R.; Heizer, C.; Albrecht, R.; Ecke, M.; Schwartz, J.-M.; Weber, I.; Gerisch, G., Three-dimensional patterns and redistribution of myosin II and actin in mitotic Dictyostelium cells. *J. Cell Biol.* **1997,** *139* (7), 1793.
34. Rappaport, R., Experiments concerning the cleavage stimulus in sand dollar eggs. *J Exp Zool* **1961,** *148* (1), 81-89.
35. Rappaport, R., Cytokinesis in Animal Cells. In *Biomechanics of Active Movement and Deformation of Cells*, Akkaş, N., Ed. Springer-Verlag: Berlin, Heidelberg, 1990; Vol. H 42, pp 1-34.
36. Field, C. M.; Alberts, B. M., Anillin, a contractile ring protein that cycles from the nucleus to the cell cortex. *J. Cell Biol.* **1995,** *131* (1), 165-178.
37. Jananji, S.; Risi, C.; Lindamulage, I. K. S.; Picard, L.-P.; Van Sciver, R.; Laflamme, G.; Albaghjati, A.; Hickson, G. R. X.; Kwok, B. H.; Galkin, V. E., Multimodal and polymorphic interactions between anillin and actin: their implications for cytokinesis. *J. Mol. Biol.* **2017,** *429* (5), 715-731.
38. Piekny, A. J.; Maddox, A. S., The myriad roles of Anillin during cytokinesis. *Sem Cell Dev Biol* **2010,** *21* (9), 881-891.
39. Kučera, O.; Janda, D.; Siahaan, V.; Dijkstra, S. H.; Pilátová, E.; Zatecka, E.; Diez, S.; Braun, M.; Lansky, Z., Anillin propels myosin-independent constriction of actin rings. *bioRxiv* **2020**, 2020.2001.2022.915256.
40. Fey, P.; Dodson, R. J.; Basu, S.; Chisholm, R. L., One stop shop for everything Dictyostelium: dictyBase and the Dicty Stock Center in 2012. In *Methods Mol Biol*, Eichinger, L.; Rivero, F., Eds. Humana Press: Totowa, NJ, 2013; pp 59-92.